XXI IMEKO World Congress "Measurement in Research and Industry"
August 30 - September 4, 2015, Prague, Czech Republic

DEGRADATION TESTS AND CHARACTERIZATION PROCEDURES OF PHOTOVOLTAIC MODULES EXPOSED TO OUTDOOR CONDITIONS

Alessio Carullo [1], *Alberto Vallan* [1], *Alessandro Ciocia* [2], *Filippo Spertino* [2]

[1] Politecnico di Torino, Dipartimento di Elettronica e Telecomunicazioni, Torino, Italy, alessio.carullo@polito.it
[2] Politecnico di Torino, Dipartimento Energia, Torino, Italy, filippo.spertino@polito.it

Abstract - This paper deals with the definition of test procedures specifically conceived to highlight the degradation of PhotoVoltaic (PV) modules and identify the mechanisms that are mainly responsible for this degradation. Several environmental and mechanical test cycles are applied to each set of PV modules under test and suitable characterization procedures are performed at the end of each test cycle, thus providing information related to the degradation rate. The applied stimuli are designed according to the measurements available for outdoor exposed PV plants and the laboratory results will be compared to the degradation estimated for these plants.

Keywords: Photovoltaic power systems, degradation, electric variables measurement, uncertainty, data acquisition

1. INTRODUCTION

The growing use of assessed PhotoVoltaic (PV) technologies for electrical energy production [1] has highlighted a lack of information that is related to the expected degradation the installed PV modules are subjected to and to the degradation mechanisms. Nameplate specifications often include the parameters that allow the initial performance of PV modules to be estimated at different operating conditions [2]-[6], but parameters that are related to the time drift of the PV module performance are hardly available. Some manufacturers provide a product warranty, e.g. 90% of the initial maximum power warranted during the first 10 years and 80% of the initial maximum power warranted during the first 25 years. However, this information does not allow the pay-back time of a plant to be reliably predicted, since the trend of the time drift is not stated and the phenomena that are mainly responsible for this degradation are not well known. Experimental results are available in literature [7]-[10] that report the actual degradation of outdoor exposed PV plant after many years of operations, but these results mainly refer to crystalline silicon modules and are based on a comparison between initial and final measurements, thus not providing any information about the degradation trend.

In a recent work [11], the authors described a data-acquisition system that has been conceived to provide traceable measurements of electrical and environmental quantities of outdoor exposed PV plants. Such a system has been put in operation since October 2010 and it is still monitoring ten plants based on different PV technologies. Starting from the acquired measurements, a preliminary estimation of the degradation of the monitored PV plants for a period of three years has been proposed in [12]. The obtained results, that are provided on a monthly basis for crystalline silicon and thin film modules, have shown a noticeable difference among technologies. In addition, worst degradations have been estimated for modules mounted on 2-axis tracking systems.

With the aim of better understanding the mechanisms that are responsible for the degradation of outdoor exposed PV modules, the authors are defining a series of laboratory tests and characterization procedures. The tests will be conceived to simulate typical outdoor conditions and obtain a convenient acceleration factor, thus minimizing the test time (accelerated or highly accelerated tests). The characterization procedures will include the estimation of the electrical parameters of the tested PV modules and the application of imaging-processing techniques that are able to identify micro-cracking and other defects that result in power-loss of PV modules.

The laboratory tests, which will be performed on new PV modules after their preliminary characterization, will be designed to simulate the outdoor thermal and mechanical stresses the monitored PV plants [11] are subjected to. Further characterizations of the tested PV modules will allow to estimate the actual degradation due to the applied stress factors. The estimated degradation will be compared with the results reported in [12], that are updated in this paper adding the results of a 16-months monitoring period.

2. PV PLANTS UNDER MONITORING

The PV plants the authors have been monitoring since October 2010 are located in Piemonte (Italy) at a latitude of about $45\ ^{\circ}\mathrm{N}$. The main results obtained for these plants in the period October 2010 - December 2014 are summarized in Table 1, where the investigated PV technologies are reported in the second column. The plants A, B, C, D, and E employ PV modules mounted in a fixed position with a tilt angle β of 35° and South oriented (azimuth angle $\gamma = 0^{\circ}$), while the modules of the plant F are mounted on the horizontal plane ($\beta = 0^{\circ}$). The other four plants employ PV modules mounted on 2-axis tracking systems: At, Dt, and Et are based on the same technology of the corresponding fixed plants, while Gt uses High Concentration PV (HCPV) modules.

Third and fourth columns in Table 1 report the results obtained during the initial characterization of the

Table 1. Results obtained for the monitored PV plants in the period October 2010-December 2014.

Plant	PV Technology	P_{act} (kW)	η_{act} (%)	$\eta_{\mathrm{rel-drift}}$ (%/year)	$U(\eta_{\mathrm{rel-drift}})$ (%/year)
A	m-Si	1.93	17.3	- 0.1	0.8
B	p-Si	1.80	12.9	- 0.05	0.8
C	String ribbon Si	2.16	12.0	-0.5	0.8
D	CIGS	1.67	9.3	- 1.6	0.8
E	CdTe	1.61	9.1	- 2.7	0.8
F	CIGS cylindrical	1.69	9.0		
At	m-Si	1.95	17.3		
Dt	CIGS	1.66	9.1	- 2.4	1.0
Et	CdTe	1.61	9.1	- 3.1	1.0
Gt	HCPV	1.55			

investigated modules in terms of actual maximum power (P_{act} expressed in kW) and PV efficiency (η_{act} expressed as a percentage). The last two columns refer to the results obtained during a monitoring period of 50 months and include the estimated relative drift of the PV efficiency ($\eta_{\mathrm{rel-drift}}$) and the corresponding expanded uncertainty ($U(\eta_{\mathrm{rel-drift}})$ obtained with a coverage factor equal to 2), which are both expressed as %/year. These results have been obtained according to the procedure described in [12] and updating the monitoring period up to December 2014, thus adding a 16-months monitoring period. The results are only reported for the plants that have shown a regular behavior in the monitored period, thus excluding the plants F, At and Gt that had problems of reliability and unexpected poor performance. Figure 1 shows an example of results that refer to the estimated PV efficiency at the Standard Test Conditions (STC: standard spectrum 1000 $\mathrm{W/m^2}$ and cell temperature 25 °C) of CIGS modules mounted in fixed position (red boxes) and on the tracking system (blue circles).

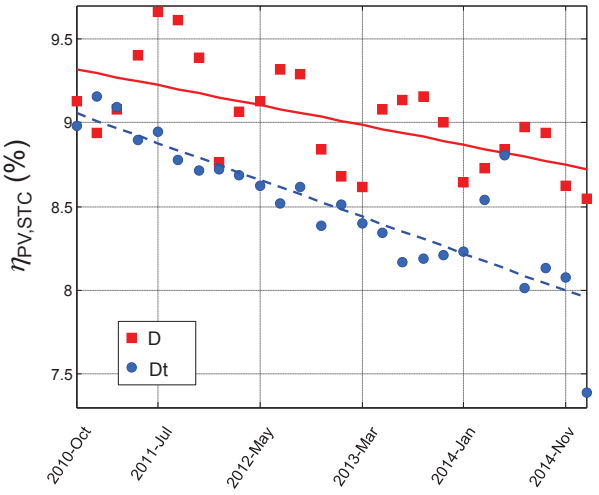

Fig. 1. Comparison between the estimated degradation of PV efficiencies at STC of plants D (red line) and Dt (dashed-blue line).

One should note that, despite the very high uncertainty of the estimated PV-efficiency relative drift, important conclusions can be made by comparing the investigated PV plants. First of all, silicon technologies show lower drift than thin-film technologies. Furthermore, m-Si and p-Si modules are less subjected to degradation that string ribbon Si modules. Another important indication of the results reported in Table 1 is the worse degradation of modules mounted on 2-axis tracking systems compared to the same modules mounted in fixed position, that suggests that the higher thermal and mechanical stresses these modules are subjected to are responsible for a fast degradation rate [13]-[15].

Starting from the results obtained through the monitoring of the PV modules exposed to outdoor conditions, the authors are designing a series of laboratory tests that are intended to better understand the degradation mechanisms. With respect to the tests suggested in the document [16], which are conceived to simulate a long-term degradation of PV modules, the tests suggested in this paper are focused on the identification of the degradation rate due to specific stresses applied to the investigated PV technologies. The main characterization procedures used to estimate the degradation rate and highlight the degradation mechanisms are based on the measurement of the electrical parameters of PV modules and on the electroluminescence technique.

3. LABORATORY TESTS

A preliminary series of test has been performed on ten p-Si modules without any embedded bypass diode: this technology has been selected because it exhibited the lowest degradation rate during the described monitoring activity. The ten PV modules are subdivided into two sets: the first one includes five modules ($P_{\mathrm{mpp}} = 10$ W) with a metallic frame and the second one includes five modules ($P_{\mathrm{mpp}} = 5$ W) encapsulated in a semi-rigid plastic frame. The main

Table 2. Mechanical and electrical characteristics of the p-Si modules under test.

Module size	305x254	395x280	mm
Cell size	57x10	75x24	mm
Strings in parallel	2	1	
Cells in series	34	36	
Frame type	semi-rigid plastic	metallic	
P_{mpp}	5	10	W
V_{mpp}	16.0	17.5	V
I_{mpp}	0.30	0.58	A
V_{oc}	20.2	22.2	V
I_{sc}	0.33	0.64	A

mechanical and electrical characteristics of the PV module under test are summarized in Table 2.

The current-voltage $I - V$ characteristic of all the tested modules has been initially obtained by means of the technique described in the section 3.1 and the maximum power of each module has been estimated at STC. The same modules have been subjected to the electroluminescence technique described in the section 3.2. Then, one module of each set has been stored and preserved by further stresses in order to act as a reference sample (sample 1), while the other four modules have been separately subjected to environmental and mechanical stresses.

The sample 2 has been exposed to damp-heat tests, i.e. tests at a high constant humidity and variable temperature that are conceived to accelerate the water adsorption and hence decrease the electrical insulation. The sample 4 has been subjected to thermal cycles in the temperature range of -20 °C to 70 °C. The figure 2 shows a picture of the tested PV modules inside the climatic chamber and temperature and humidity profiles during the 24-hour damp-heat test.

The last two samples are mechanically stressed: sample 5 will be subjected to cycles of static loads, while sample 3 has been subjected to dynamic loads. The latter condition has been obtained by mounting the sample on the vibrating table of an electrodynamic shaker, as shown in the figure 3 that refers to the test performed on the flexible PV module. The electrodynamic shaker has been driven in order to perform random vibration cycles in the frequency range of 5 Hz to 150 Hz. The figure 3 shows the acceleration spectral density that corresponds to a root mean square acceleration of 5 $\mathrm{m/s^2}$ of a 5-hour test.

At the end of each test cycle, the $I - V$ characteristic of the investigated samples are again obtained in order to highlight possible power losses, which are considered meaningful if their values are greater than the measurement uncertainty. When important power losses will be observed, the EL image of each PV module will be obtained in order to identify the mechanisms that are responsible for the module degradation. In addition, the insulation resistance of each sample will be measured.

3.1. Current-voltage measurement

The measurement of the $(I - V)$ characteristic is a valid tool to continuously monitor the operation of an array of PV modules. Among the available methods, the capacitive-load based technique has been adopted here, simultaneously detecting voltage, current, irradiance and temperature [5], [17]. In general, $I - V$ measurements or the scanning for MPPT must be carried out at constant ambient conditions (irradiance and temperature): according to [18], the maximum duration for the charging transient is 100 ms. However, to trace the $I - V$ curve in an accurate way, minimizing the effect of parasitic parameters [19], it is recommended to choose capacitances so that the total test time is greater than 20 ms. According to this requirement, the used capacitances range from 0.5 mF to 1 mF. The next data-processing to achieve the STC parameters is performed by a conventional correction method [20]. The measurement uncertainties ensured by the system used by the authors are summarized below:

- for the irradiance G the absolute uncertainty is ± 20 $\mathrm{W/m^2}$, for the air temperature T_{a} the absolute uncertainty is ± 0.2 °C, for the cell temperature T_{cell} the absolute uncertainty is ± 2 °C (indirect measurement obtained with open circuit voltage and its thermal coefficient [21]-[22]);
- for the short circuit current I_{sc}, the open-circuit voltage V_{oc} and the maximum power P_{M} of the PV generator, the corresponding relative uncertainties are $\pm 2\%$, $\pm 0.1\%$ and $\pm 2.1\%$;
- for the fill factor FF, defined as the ratio of the maximum power P_{M} to the product $V_{\mathrm{oc}} \cdot I_{\mathrm{sc}}$, the relative uncertainty is $\pm 4\%$;
- for the maximum power at STC $P_{\mathrm{mpp}} = V_{\mathrm{mpp}} \cdot I_{\mathrm{mpp}}$, the relative measurement uncertainty is $\pm 6\%$.

3.2. Electroluminescence

Electroluminescence (EL) is a non-destructive testing technique, which allows the most common defects in a PV module to be detected with high resolution. Applying a forward bias to a totally shaded PV generator, it works like a LED (Light Emitting Diode). Unlike the semiconductor materials used in LEDs, the emission spectra from PV generators in crystalline silicon cells is not in the visible region of the electromagnetic spectrum. The luminescence signal ranges from about 950 nm to about 1350 nm and the peak, corresponding to the band gap, is of 1150 nm [23]. The emitted photons can be detected with a sensitive camera equipped with silicon charge-coupled device (CCD) or indium gallium arsenide (InGaAs) photodiodes. During EL tests, solar cells or PV modules are supplied with an external excitation current lower than the short circuit current of the generator and the camera takes an image. Defective areas appear darker than perfect areas. In [24] the influence of external excitation current in EL tests is investigated: low

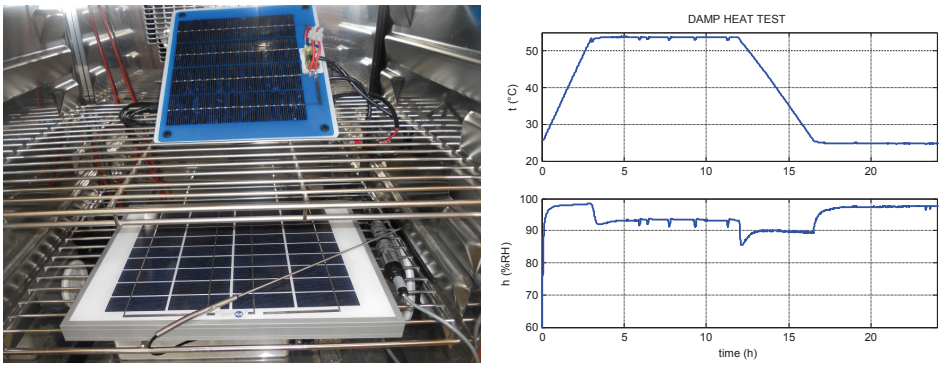

Fig. 2. A picture of the tested PV modules (sample 2 of each set) inside the climatic chamber (on the left) and temperature and humidity profiles during the 24-hour damp-heat test (on the right).

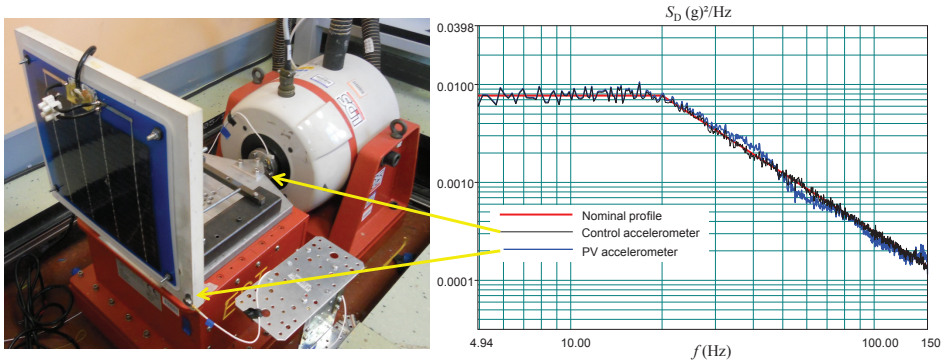

Fig. 3. A picture of the flexible PV module (sample 3) on the electrodynamic shaker (on the left) and acceleration spectral density during the test (on the right).

current densities permit to study the material properties; high values are used to test the properties of the electrical contacts. Moreover, in order to obtain an accurate image, a high signal to noise ratio must be maintained, cutting off all sources of light. Hence, to avoid any kind of reflection, tests should be performed inside a darkroom.

EL analysis is able to detect different types of defects that may occur during the single phases of the life of PV modules (i.e. production stage, transport, installation). Several defects can be highlighted by means of EL, such as:

- micro cracks, which are generated during the cell and module production, that are due to mechanical or thermal stresses and can evolve into broken cells;
- broken cells, which are characterized by electrically isolated areas limiting the current in the whole string, that are one of the main sources of power loss;
- impurities and chain pattern, which appear in EL pictures like less shine areas, that are due to low quality production processes;
- Potential Induced Degradation (PID), which is a mechanism caused by a leakage current depending on high voltage with respect to earth and weather conditions (high temperature and humidity).

4. PRELIMINARY RESULTS

The initial measured $I-V$ curve on PV modules with metallic frame has shown a good conformity with respect to the nameplate specifications: the estimated maximum power at STC was higher (in the range of $+1$ % to $+2$ %) than the same parameter stated by the manufacturer, as highlighted in Table 3 that summarizes the results of the electrical characterization for modules with metallic frame (items m-i) and with plastic frame (items p-i). On the contrary, modules with plastic frame have shown significant lower performance with respect to the nameplate specifications, with difference in the maximum power at STC that reaches -21% for the module p-5. Figure 4 shows an example of $I-V$ and $P-V$ curves of the PV module m-2 at the actual conditions of irradiance and temperature and at STC.

The EL images of modules with metallic frame have shown few cracks and micro-cracks. Nevertheless, there are many interrupted fingers and small isolated areas, probably due to shocks during assembly. The most interesting point is the presence of a strong non-uniformity luminescence within many cells and between all the cells forming the module, which means a strong $I-V$ mismatch. It is because PV modules are assembled with piece of solar cells with higher surface, usually they are wasted cells. The figure 5-(a) shows

Table 3. Initial electrical characteristics measured for the PV modules under test (m-i refers to modules with metallic frame, while p-i refers to modules with plastic frame).

Quantity	m-1	m-2	m-3	m-4	m-5	p-1	p-2	p-3	p-4	p-5	unit
G	854	930	903	875	912	902	969	927	974	920	$\mathrm{W/m^2}$
T_{cell}	49	49	50	48	51	52	54	53	55	53	$^{\circ}\mathrm{C}$
P_{M}	7.81	8.54	8.13	7.94	8.15	4.13	3.57	3.36	3.76	3.08	W
V_{Pmax}	15.36	16.02	15.71	15.67	15.77	14.12	14.53	14.68	14.80	14.32	V
V_{oc}	20.17	20.49	20.23	20.35	20.11	18.22	18.09	18.13	18.16	18.14	V
I_{Pmax}	0.51	0.53	0.52	0.51	0.52	0.29	0.25	0.23	0.25	0.22	A
I_{sc}	0.55	0.58	0.58	0.55	0.57	0.32	0.32	0.26	0.29	0.30	A
FF	0.71	0.72	0.69	0.71	0.71	0.71	0.61	0.72	0.71	0.57	
P_{mpp} @ STC	10.2	10.2	10.1	10.1	10.2	5.22	4.29	4.17	4.47	3.95	W
V_{mpp} @ STC	17.45	17.84	17.38	16.94	17.71	15.70	16.02	16.53	17.06	16.13	V
I_{mpp} @ STC	0.58	0.57	0.58	0.60	0.57	0.33	0.27	0.25	0.26	0.25	A

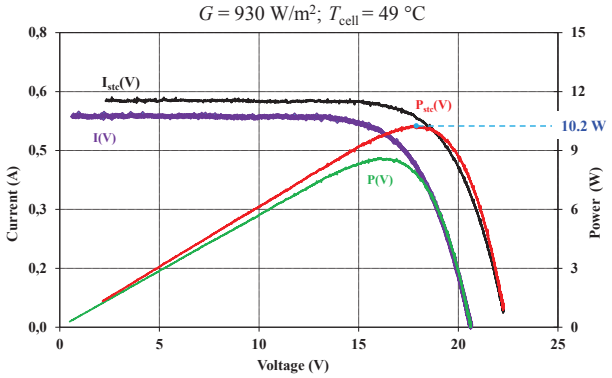

Fig. 4. $I-V$ and $P-V$ curves of the PV module m-2 at the actual conditions of irradiance and temperature and at STC.

the electroluminescence image of one of the modules with metallic frame: there are at least two cells with performance well below the other ones. During the assembly process, a selection of the cells can decreases the "bottleneck" effect and the PV module can produce more power.

Thanks to electroluminescence analysis, a strong $I-V$ mismatch is also evident in the cells forming the modules with plastic semi-rigid frame, as a result of using wasted cells. However, in this case, the power loss with respect to the nameplate specifications is due to the presence of many isolated parts of cells, cracks and micro-cracks. The EL image in figure 5-(b) shows these defects in one of the modules with high power losses.

Once the initial characterization of the two sets of PV modules under test has been completed, the first stress tests have been performed. The samples 2 have been subjected to a 24-hour damp-heat test according to the profile of figure 2, while the samples 4 have been subjected to a 24-hour thermal-cycle test in the temperature range of $-20\ ^{\circ}\mathrm{C}$ to $70\ ^{\circ}\mathrm{C}$. The samples 3 of both sets have been subjected to a 5-hour random vibration cycle in the frequency range of 5 Hz to 150 Hz with a root mean square acceleration of $5\ \mathrm{m/s^2}$ according to the spectral distribution of figure 3. After these first tests, the $I-V$ curves of the modules subjected to stress and of the reference samples have been obtained again at constant conditions of temperature and irradiance and then corrected to be related to the STC. The comparison between pre-stress and post-stress parameters (above all P_{mpp} @ STC) has not shown meaningful differences, thus indicating the need to increase the level of stress (amplitude and/or duration) in order to be able to correlate the applied stress factor to the observed degradation.

5. CONCLUSIONS

This paper presents an attempt of defining tests that are able to identify the factors that are mainly responsible for degradation of PV modules exposed to outdoor conditions. A preliminary test-protocol has been proposed and suitable characterization procedures have been described. Preliminary tests have been performed that have involved PV modules made up of p-Si cells with metallic and plastic frames. The first results have not shown significant differences between pre-stress and post-stress conditions. Authors are now performing further stress tests on the PV modules and the corresponding results will be presented at the conference. In addition, PV modules based on different technologies will be tested with the proposed procedure.

REFERENCES

[1] International Energy Agency, Photovoltaic Power Systems Programme, A Snapshot of Global PV 19922012, Preliminary information, Report IEA-PVPS T1-22, 2013.

[2] J.A. Gow and C.D. Manning, "Development of a photovoltaic array model for use in power-electronics simulation studies", *IEE Electric Power Appl.* vol. 146, n^o 2, pp. 193-200, 1999.

[3] F. Adamo, F. Attivissimo, A. Di Nisio and M. Spadavecchia, "Characterization and testing of a tool for photovoltaic panel modeling", *IEEE Trans. Instr. Meas.*, vol. 60, n^o 5, pp. 1613-1622, 2011.

[4] S. Ubertini and U. Desideri, "Performance estimation and experimental measurements of a photovoltaic roof", *Renew.*

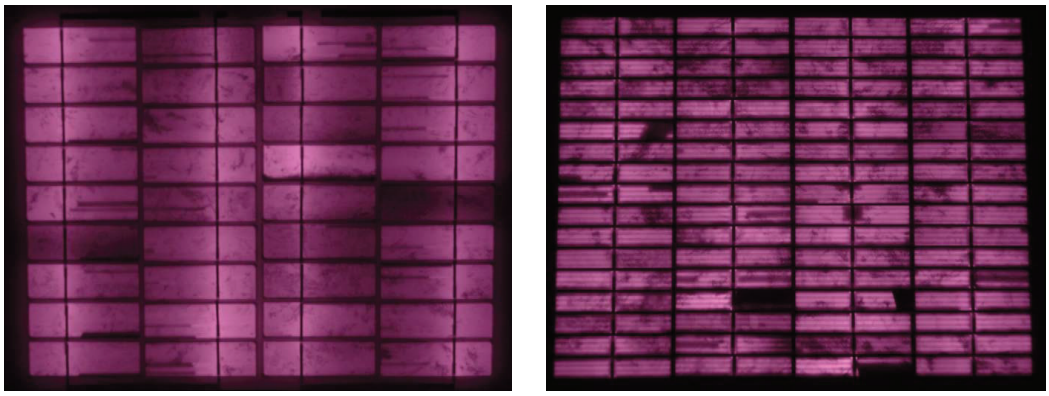

(a) (b)

Fig. 5. Examples of EL images of a PV module with metallic frame (a) and with plastic semi-rigid frame (b).

Energy, vol. 28, pp. 1833-1850, 2003.

[5] F. Attivissimo, F. Adamo, A. Carullo, A.M.L. Lanzolla, F. Spertino and A. Vallan, "On the performance of the double-diode model estimating the maximum power point for different photovoltaic technologies", *Measurement*, vol. 46, n^o 3, pp. 3549-3559, 2013.

[6] F. Spertino, F. Corona and P. Di Leo, "Limits of advisability for masterslave configuration of DC-AC converters in photovoltaic systems", *IEEE J. Photovolt.*, vol. 2, n^o 4, pp. 547-554, 2012.

[7] E.D. Dunlop and D. Halton, "The performance of crystalline silicon photovoltaic solar modules after 22 years of continuous outdoor exposure", *Prog. Photovolt.: Res. Appl.*, vol. 14, pp. 53-64, 2006.

[8] A. Skoczek, T. Sample and E.D. Dunlop, "The results of performance measurements of field-aged crystalline silicon photovoltaic modules", *Prog. Photovolt.: Res. Appl.*, vol. 17, pp. 227-240, 2009.

[9] D.C. Jordan and S.R. Kurtz, "Photovoltaic degradation rates an analytical review", *Prog. Photovolt.: Res. Appl.*, vol. 21, pp. 12-29, 2013.

[10] E. Lorenzo, R. Zilles, R. Moreton, T. Gomez and A. Martinez de Olcoz, "Performance analysis of a 7-kW crystalline silicon generator after 17 years of operation in Madrid", *Prog. Photovolt.: Res. Appl.*, 2013, http://dx.doi.org/10.1002/pip.2379.

[11] A. Carullo and A. Vallan, "Outdoor Experimental Laboratory for Long-Term Estimation of Photovoltaic-Plant Performance", *IEEE Trans. on Instrum. and Meas.*, vol. 61, n^o 5, pp. 1307-1314, 2012.

[12] A. Carullo, F. Ferraris, A. Vallan, F. Spertino and F. Attivissimo, "Uncertainty analysis of degradation parameters estimated in long-term monitoring of photovoltaic plants", *Measurement*, vol. 55, pp. 641-649, 2014, http://dx.doi.org/10.1016/j.measurement.2014.06.003.

[13] M. Paggi, M. Corrado and M.A. Rodriguez, "A multi-physics and multi-scale numerical approach to microcracking and power-loss in photovoltaic modules", *Composite Structures*, vol. 95, pp. 630-638, 2013.

[14] G. Makrides, B. Zinsser, A. Phinikarides, M. Schubert and G.E. Georghiou, "Temperature and thermal annealing effects on different photovoltaic technologies", *Renewable Energy*, vol. 43, pp. 407-417, July 2012.

[15] J. Schlothauer, S. Jungwirth, M. Köhl and B. Röder, "Degradation of the encapsulant polymer in outdoor weathered photovoltaic modules: spatially resolved inspection of EVA ageing by fluorescence and correlation to electroluminescence", *Solar Energy Materials & Solar Cells*, vol. 102, pp. 75-85, 2013.

[16] Standard IEC 61215:2005-04, *Crystalline silicon terrestrial photovoltaic (PV) modules - Design qualification and type approval.*

[17] F. Spertino, J. Sumaili, H. Andrei, G. Chicco, "PV module parameter characterization from the transient charge of an external capacitor," *IEEE Journal of Photovoltaics*, vol. 3, 2013, pp. 1325-1333.

[18] Commission of the European Communities, Joint Research Centre, *Guidelines for the Assessment of Photovoltaic Plants - Initial and Periodic Tests on PV Plants, Document C*, European Commission Joint Research Centre, Ispra, Italy, 1995.

[19] F. Spertino, J. Ahmad, A. Ciocia, P. D. Leo, A. F. Murtaza, M. Chiaberge, "Capacitor charging method for I-V curve tracer and MPPT in photovoltaic systems," *Solar Energy*, 2015.

[20] Standard IEC 60891:2009-12, *Photovoltaic devices - Procedures for temperature and irradiance corrections to measured I-V characteristics.*

[21] F. Spertino, A. Ciocia, F. Corona, P. Di Leo, F. Papandrea, "An experimental procedure to check the performance degradation on-site in grid-connected photovoltaic systems," *40th IEEE Photovoltaic Specialists Conference (PVSC)*, pp. 2600-2604, 2014.

[22] EN Standard 61829:1998, *Crystalline silicon photovoltaic (PV) array: on-site measurement of I-V characteristics.*

[23] Fuyuki, Takashi and Kondo, Hayato and Yamazaki, Tsutomu and Takahashi, Yu and Uraoka, Yukiharu, "Photographic surveying of minority carrier diffusion length in polycrystalline silicon solar cells by electroluminescence", *Applied Physics Letters*, vol. 86, 2005.

[24] R. Ebner, B. Kubicek and G. Ujvari, "Non-destructive techniques for quality control of PV modules: infrared thermography, electro- and photoluminescence imaging", *Industrial Electronics Society - 39th Annual Conference of the IEEE*, pp. 8104-8109, 2013.